PLANT SCIENCE TODAY
Vol x(x): xx–xx
https://doi.org/10.14719/pst.13910

eISSN 2348-1900

RESEARCH ARTICLE

Proteomic insights into ultraviolet-B stress adaptation in *Mimosa pudica* L. and *Senna auriculata* L. Roxb.

Shanthi Natarajan[1*], Pillathil Jegan Pillathil Senthil Mani[1], Selvakumar Murugan[1], IndiraRani Selvaraj[2], Ragunathan Vinoth Kumar[2] & Murugesan Subbiah[1]

[1]PG and Research Department of Botany, Pachaiyappa's College (Affiliated to University of Madras), Chennai 600 030, Tamil Nadu, India
[2]PG and Research Department of Botany, V.O. Chidambaram College (Affiliated to Manonmaniam Sundaranar University, Tirunelveli), Tuticorin 628 008, Tamil Nadu, India

*Correspondence email - prithishanthi@gmail.com

Received: 30 January 2026; Accepted: 20 May 2026; Available online: Version 1.0: 04 August 2026

Cite this article: Shanthi N, Pillathil JPSM, Selvakumar M, IndiraRani S, Ragunathan VK, Murugesan S. Proteomic insights into ultraviolet-B stress adaptation in *Mimosa pudica* L. and *Senna auriculata* L. Roxb. Plant Science Today (Early Access). https://doi.org/10.14719/pst.13910

Abstract

Differential proteomic responses of *Mimosa pudica* L. and *Senna auriculata* L. Roxb. under ultraviolet-B (UV-B) radiation were examined using sodium dodecyl sulfate-polyacrylamide gel electrophoresis (SDS-PAGE) and two-dimensional gel electrophoresis (2-DE). Under normal conditions, both species exhibited stable and comparable protein expression patterns. However, UV-B exposure induced distinct, species-specific proteomic alterations. *Senna auriculata* showed an early and sustained upregulation of stress-responsive proteins, indicating rapid activation of defence and protective mechanisms. In contrast, *M. pudica* displayed a delayed proteomic response, with changes becoming evident only at later stages of exposure. Both species exhibited a reduction in low molecular weight proteins, suggesting a metabolic shift from growth-related processes to stress adaptation. Overall, the findings highlight that *S. auriculata* possesses a more efficient and timely proteomic response to UV-B stress than *M. pudica*, providing valuable insights into the molecular basis of plant resilience under environmental stress conditions.

Keywords: *Mimosa pudica*; molecular chaperones; oxidative stress; photosystem II; proteomic profiling; redox regulation; *Senna auriculata;* sodium dodecyl sulfate-polyacrylamide gel electrophoresis; two-dimensional gel electrophoresis; ultraviolet-B-induced oxidative damage

Introduction

Ultraviolet-B (UV-B) radiation (280–315 nm) is one of the components of solar radiation that has become an important environmental stressor for plant growth, physiology and metabolism. With ozone depletion and global change, plants receive increasingly high levels of UV-B, which interfere with cellular homeostasis by causing DNA damage, lipid peroxidation, oxidative stress and impairment of photosynthetic processes (1, 2). Plants initiate complex protective mechanisms to overcome these effects, including the sequestration of protective pigments such as flavonoids and large-scale reprogramming of their proteomic and metabolic pathways to mitigate UV-B-induced damage (3, 4).

Proteomic approaches have proven to be powerful tools for elucidating plant molecular responses to abiotic stress. Sodium dodecyl sulfate-polyacrylamide gel electrophoresis (SDS-PAGE) and two-dimensional gel electrophoresis (2-DE) enable the resolution and comparative quantification of stress-responsive proteins. While SDS-PAGE primarily separates proteins based on molecular weight, allowing the detection of broad expression changes, 2-DE provides higher resolution by separating proteins according to both isoelectric point and molecular mass, facilitating the detection of protein isoforms and post-translational modifications (5, 6). These techniques play an important role in identifying proteins involved in stress perception, signal transduction, redox regulation and cellular protection mechanisms, thereby contributing to our understanding of plant adaptation to UV-B stress (1–6). However, these gel-based approaches alone do not allow precise protein identification without complementary mass spectrometry techniques.

Mimosa pudica L. is a tropical legume widely recognised for its rapid thigmonastic leaf-folding response, driven by ion fluxes and turgour changes and is frequently used as a model for studying plant sensory perception and stress signalling (7, 8). Ecologically, it predominately occurs in disturbed or semi-shaded habitats where prolonged exposure to intense solar radiation and UV-B stress is limited and previous studies indicate a relatively low tolerance to sustained oxidative and radiation stress (9, 10).

Senna auriculata L. Roxb., is a medicinal shrub native to arid and semi-arid regions, naturally adapted to open habitats characterised by high solar irradiance and chronic photooxidative stress (11). It's reported high basal antioxidant capacity, elevated phenolic and flavonoid content and enhanced abiotic stress tolerance suggest an inherent ability to withstand UV-B-induced damage, making it an appropriate comparative species for this study (12, 13).

In the present study, SDS-PAGE and 2-DE were employed to characterise UV-B-induced proteomic changes in *M. pudica* and

S. auriculata. The results revealed distinct differences in both the timing and magnitude of protein regulation between the two species: *S. auriculata* exhibited a rapid and robust induction of stress-responsive proteins, whereas *M. pudica* showed delayed but cumulative proteomic remodelling. These findings provide new insights into plant adaptive strategies and stress memory and highlight the potential application of proteomic markers in breeding programmes aimed at improving UV-B resilience, as well as advancing molecular understanding of plant-environment interactions.

Materials and Methods

Plant material and UV-B treatment

Plant material

Certified seeds of *M. pudica* and *S. auriculata*, both recognised for their medicinal significance, were obtained from a reputable commercial supplier in Chennai, Tamil Nadu. The seeds were germinated and cultivated in the Botanical Garden of the Department of Botany at Pachaiyappa's College, Chennai, India, during February 2024. The seedlings were divided into two groups, one maintained under natural ambient sunlight as the control and the other subjected to enhanced UV-B radiation.

Kingdom	Plantae	Plantae
Division	Angiosperms	Angiosperms
Class	Eudicots	Fabales
Order	Fabales	Fabaceae
Family	Fabaceae	Fabaceae
Subfamily	Mimosoideae	Mimosoideae
Genus	*Senna*	*Mimosa*
Species	*auriculata*	*pudica*

Seed germination and growth conditions

To enhance germination rates, seeds were soaked in running water for 6–7 hr prior to sowing. The seeds were then sown in well-prepared soil beds under open-field conditions. Separate plots were designated for the control and UV-B treatment groups. In total, four plots were established: two plots exposed to natural sunlight (control) and two plots subjected to supplemental UV-B radiation, with each plot containing 20 seeds.

Seedlings were irrigated regularly to maintain optimal soil moisture and standard horticultural practices were followed to minimise microbial infection and pest infestation. Throughout the experimental period, the plants were grown under ambient environmental conditions, with average daytime temperatures ranging between 30 °C and 36 °C, relative humidity between 65 % and 85 % and a natural photoperiod of approximately 12 hr light/ 12 hr dark. Photosynthetically active radiation (PAR) during midday ranged from 1400 to 2000 µmol m^{-2} s^{-1}. UV-B treatment was initiated once the seedlings reached the early foliar stage, characterised by the emergence of the first fully expanded true leaves.

Ultraviolet-B exposure protocol

UV-B treatment was applied using a Philips TL40W/12 sunlamp (Gloelampenfabrieken, Holland). Plants were exposed to supplemental UV-B radiation for 1 hr daily, from 11:00 a.m. to 12:00 p.m., in addition to natural sunlight, resulting in a 20 % increase in UV-B levels compared to ambient conditions. However, no matrix-assisted laser desorption/ionisation-time-of-flight mass spectrometry (MALDI-TOF) or liquid chromatography-tandem mass spectrometry (LC-MS/MS)-based protein identification of differential spots was performed, thereby limiting precise protein identification and functional characterisation. The duration of exposure and sampling intervals (including Day 10) were standardised and consistently applied across all experimental sets.

The first fully developed leaves were harvested at designated intervals following the onset of UV-B treatment. These samples were then analysed through physiological, biochemical and phytochemical assays to evaluate the plants' metabolic responses to elevated UV-B radiation.

Sampling strategy and rationale

Leaf samples were collected at 20, 30 and 40 days after the initiation of UV-B exposure. These time points were selected to capture intermediate (Days 20 and 30) and prolonged (Day 40) physiological and metabolic responses, enabling assessment of both sustained stress effects and longer-term acclimation to enhanced UV-B radiation.

At each sampling point, the first fully expanded leaves were harvested, immediately processed or appropriately stored and used for physiological, biochemical and phytochemical analyses to evaluate the dynamic metabolic responses of the plants to UV-B stress.

Measurement of radiation

Ultraviolet-B radiation intensity was measured using a UVP UVX Radiometer equipped with a UVX-31 sensor, which is specifically designed for the 280–340 nm UV-B range. During the exposure period, the intensity was maintained at approximately 1.6 W/m^2, representing a 20 % increase over ambient UV-B levels. Measurements were taken daily to ensure consistent radiation intensity throughout the experiment.

Isolation of chloroplast proteins from plant leaves

Fresh, healthy leaves were harvested, washed thoroughly with distilled water and blotted dry. All subsequent steps were carried out at 4 °C unless otherwise stated. Approximately X g of leaf tissue was homogenised in an ice-cold chloroplast isolation buffer containing 50 mM tris(hydroxymethyl) aminomethane hydrochloride (Tris-HCl) (pH 7.8), 0.33 M sorbitol, 2 mM ethylenediaminetetraacetic acid (EDTA), 5 mM magnesium chloride ($MgCl_2$) and 1 mM phenylmethylsulfonyl fluoride (PMSF) using a pre-chilled mortar and pestle. The homogenate was filtered through two layers of muslin cloth followed by one layer of nylon mesh to remove debris. The filtrate was centrifuged at 1000 × g for 5 min to remove unbroken cells and nuclei. The supernatant was then centrifuged at 3000 × g for 10 min to pellet crude chloroplasts. The chloroplast pellet was gently resuspended in the isolation buffer and centrifuged again at 3000 × g for 5 min to improve purity. The resulting pellet, containing intact chloroplasts, was used for protein extraction.

To extract soluble proteins from chloroplasts and associated membranes, isolated chloroplasts were treated with 10 % ice-cold trichloroacetic acid (TCA) and incubated on ice for 10 min to precipitate proteins. The suspension was centrifuged at 3000 × g for 5 min and the resulting protein pellet was collected. To remove residual TCA and pigments, the pellet was washed three times with ice-cold acetone followed by a wash with cold

diethyl ether. The pellet was dried under a stream of nitrogen and resuspended in 2 % SDS for subsequent analysis.

Protein estimation

Protein concentration was quantified using the Lowry method, as described by Lowry et al. (14).

Sodium dodecyl sulfate-polyacrylamide gel electrophoresis

Protein separation was carried out using SDS-PAGE according to the protocol established by Laemmli (15), employing a 10 % resolving gel and a 5 % stacking gel.

Gel composition

- Separating gel (10 %): 1.5 M Tris-HCl (pH 8.8), acrylamide/bisacrylamide, SDS, distilled water, glycerol.
- Stacking gel (5 %): 0.5 M Tris-HCl (pH 6.8), acrylamide/bisacrylamide, SDS, distilled water, ammonium persulfate (APS), N,N,N′,N′-tetramethylethylenediamine (TEMED).

A total of 300 µg of protein was mixed with sample buffer, boiled at 100 °C for 2 min and subsequently loaded onto the gel. Electrophoresis was conducted using Tris-Glycine-SDS running buffer, starting at 60 V and gradually increased to 120 V. Upon completion of protein separation, the gels were stained with silver nitrate for visualisation, following the method in previous study (16). No MALDI-TOF/MS or LC-MS/MS analysis was performed for protein identification; therefore, band identification was based solely on molecular weight estimation.

Two-dimensional gel electrophoresis analysis

For two-dimensional gel electrophoresis, proteins were extracted from 1 g of leaf tissue using an extraction buffer composed of 7 M urea, 2 M thiourea, 4 % 3-[(3-cholamidopropyl)dimethylammonio] -1-propanesulfonate (CHAPS) and 25 mM dithiothreitol (DTT). Protein precipitation was carried out using TCA and acetone. The resulting protein pellet was resuspended in 200 µL of 25 mM ammonium bicarbonate.

Rehydration

For isoelectric focusing (IEF), 30 µL of the solubilised protein sample was applied to immobilised pH gradient (IPG) strips (pH 3–10, 17 cm). Isoelectric focusing was performed under a programmed voltage gradient to achieve efficient separation based on the isoelectric point. Following IEF, the second dimension of separation was carried out using SDS-PAGE. Proteins were visualised through silver staining and gel images were analysed using ImageMaster 2D Platinum 7.0 software.

Experimental replication

All SDS-PAGE and 2-DE experiments were performed using three independent biological replicates, each with two technical repeats, to ensure reproducibility.

Statistical analysis

Data were expressed as mean ± standard deviation (SD). Statistical comparisons between control and UV-B-treated samples were performed using Student's *t*-test and analysis of variance (ANOVA), as appropriate. Differences were considered statistically significant at $p \leq 0.05$. All statistical analyses were conducted using GraphPad Prism 9 (GraphPad Software).

Results

The SDS analysis of chloroplast proteins from *M. pudica* and *S. auriculata* exposed to UV-B stress and their respective controls revealed distinct species-dependent and exposure-dependent alterations in chloroplast protein abundance (Figs. 1 and 2). Each experiment was repeated three times with independent biological samples. The intensity of the bands was quantified densitometrically and the results were expressed as mean ± SD. Statistical significance was evaluated using Student's *t*-test ($p \leq 0.05$) and a significant interaction between species and treatment duration was also detected with two-way ANOVA ($p \leq 0.05$), indicating species-specific temporal proteomic strategies.

In control samples of both species, protein banding patterns remained relatively stable throughout the experimental period, with no statistically significant variation in major bands ($p > 0.05$), reflecting normal protein turnover under non-stress

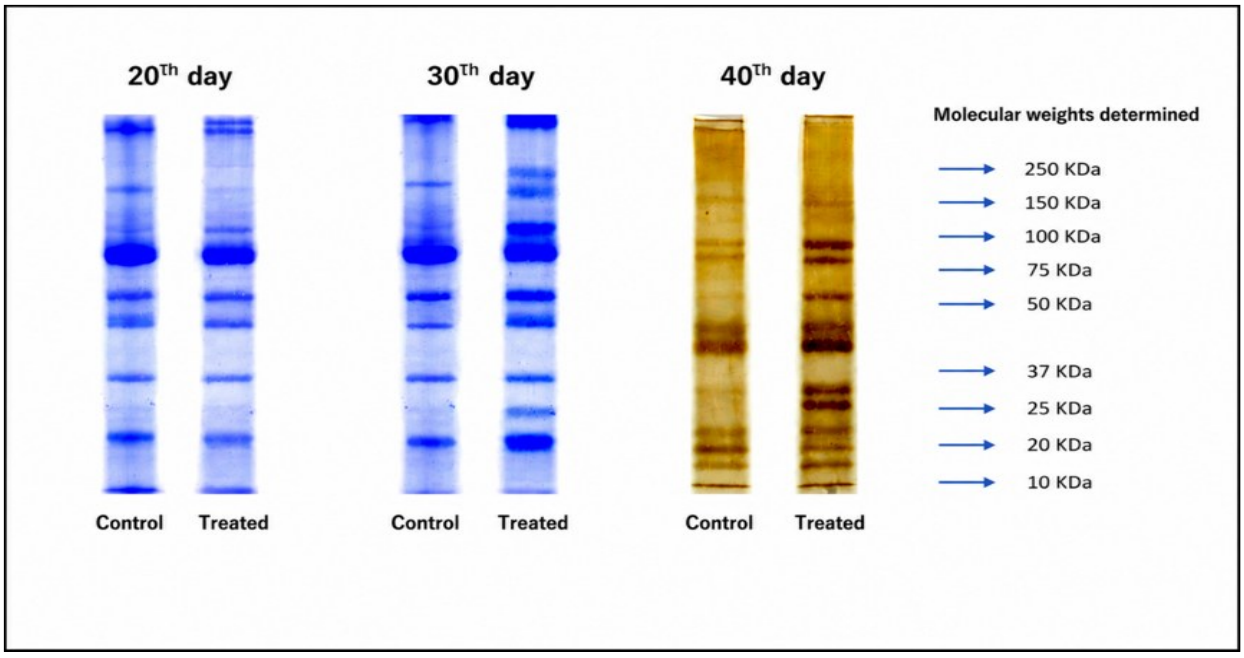


Fig. 1. Sodium dodecyl sulfate-polyacrylamide gel electrophoresis profile chloroplast polypeptides of *Mimosa pudica* plant grown under control and enhanced ultraviolet-B radiation. Protein sample equivalent to 300 µg were loaded in each well. Other details are provided in the Materials and Methods section.

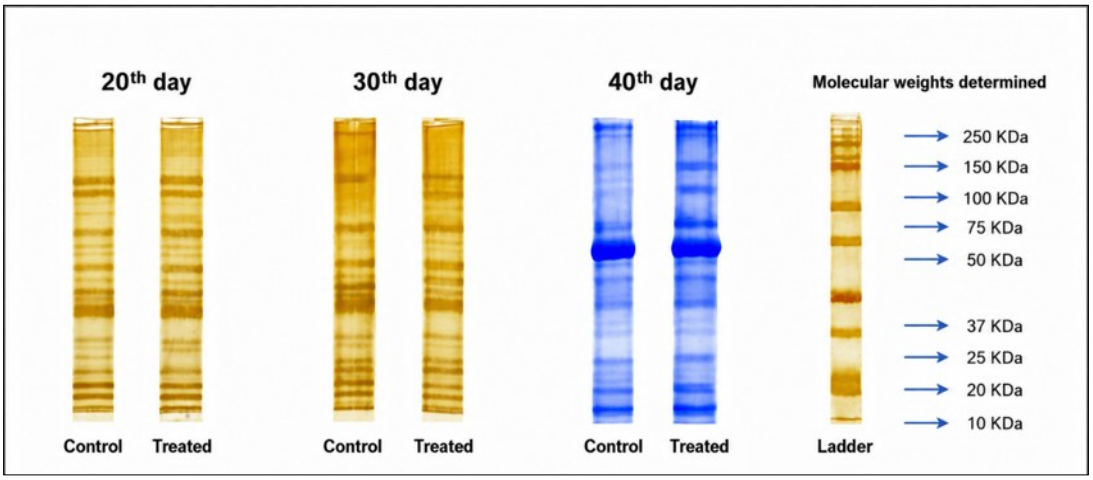


Fig. 2. Sodium dodecyl sulfate-polyacrylamide gel electrophoresis profile of chloroplast polypeptides in *Senna auriculata* plants grown under control and ultraviolet-B radiation conditions. Protein samples (300 µg per well) were loaded for each treatment. Additional methodological details are provided in the Materials and Methods section.

conditions. In *S. auriculata*, control plants consistently showed strong bands in the 10–15 kDa region, presumably representing constitutive low-molecular-weight proteins such as ribosomal peptides, light-harvesting components, pathogenesis-related peptides and other housekeeping enzymes essential for basal metabolic maintenance. Similarly, *M. pudica* controls plants exhibited stable protein profiles for at least 20 days, confirming the absence of stress-induced proteomic modulation.

Under UV-B exposure, however, distinct interspecific differences emerged. In *S. auriculata*, significant proteomic alterations were evident by Day 20. The 50 kDa region showed a 1.8-fold increase in intensity relative to the control ($p \leq 0.05$), likely corresponding to abundant chloroplast proteins such as the large subunit of ribulose-1,5-bisphosphate carboxylase/oxygenase (RuBisCO) or adenosine triphosphate (ATP) synthase β-subunit, both central to carbon fixation and energy metabolism. Significantly upregulated bands in the 37–39 kDa and 32–34 kDa regions (1.6-fold and 1.5-fold increases, respectively; $p \leq 0.05$) may correspond to the accumulation of photosystem II (PSII) core (D1/D2) proteins, Cu/Zn-superoxide dismutases (SOD) or other chloroplast stress-related enzymes. Increased intensity around 25 kDa (1.7-fold increase, $p < 0.05$) possibly reflects an increase in the abundance of proteins such as oxygen-evolving complex members required for photosystem stability. At Day 30, proteins were substantially induced in the 15–20 kDa region (2.1-fold up-regulation; $p \leq 0.01$), potentially corresponding to glutathione S-transferases (GSTs), small heat shock proteins (sHSPs) or other redox-regulated enzymes, indicating the early induction of antioxidant and chaperone-mediated defence pathways.

In contrast, *M. pudica* exhibited delayed proteomic adaptation. Changes observed on Day 20 were marginal and statistically insignificant ($p > 0.05$). Significant increases, however, were detected on Days 30 and 40 in the 60–75 kDa (1.9-fold; $p \leq 0.05$), 40–50 kDa (1.6-fold; $p \leq 0.05$) and 25–30 kDa (1.4-fold; $p \leq 0.05$). These molecular weight ranges may correspond to stress-related proteins such as HSP70/HSP90 families, ascorbate peroxidase, dehydroascorbate reductase, thioredoxins and other redox-regulating enzymes. In contrast to *S. auriculata*, the early induction of 15–20 kDa proteins were not statistically significant, indicating a delay in the activation of primary antioxidant defences. The broader induction observed at later stages suggests a cumulative and more extensive proteomic adjustment rather than a rapid, targeted response.

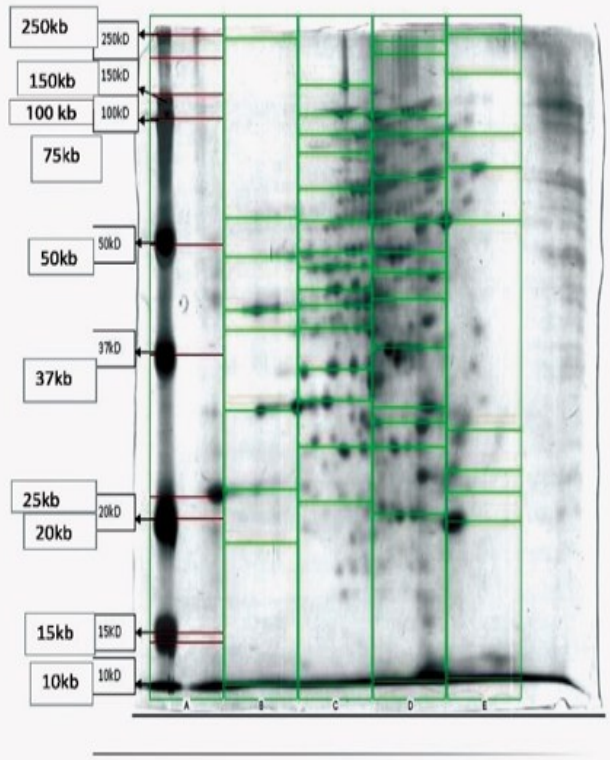
Interestingly, both taxa exhibited a marked reduction, or even complete loss, of 10–15 kDa proteins that were present under control conditions. This decline likely reflects the downregulation of small peptides and structural proteins associated with growth, indicating a metabolic shift in cellular resource allocation from primary metabolism and growth toward stress adaptation. These proteins may have included ribosomal subunits, light-harvesting complex peptides and small signalling molecules that are less utilised during oxidative stress. However, the identities of these protein bands were not confirmed using MALDI-TOF or LC-MS/MS techniques.

In general, SDS-PAGE profiling demonstrates a clear difference between the two species: specific stress-responsive proteins were induced in an early and targeted manner in *S. auriculata* and in a delayed but broader manner in *M. pudica*. Under UV-B stress, both species exhibited a time and magnitude-dependent suppression of low-molecular-weight growth-related proteins and an increase in defence-related proteins. These results demonstrate contrasting adaptive responses and possibly different levels of UV-B tolerance in the two medicinal legumes.

Two-dimensional gel electrophoresis comparative analysis

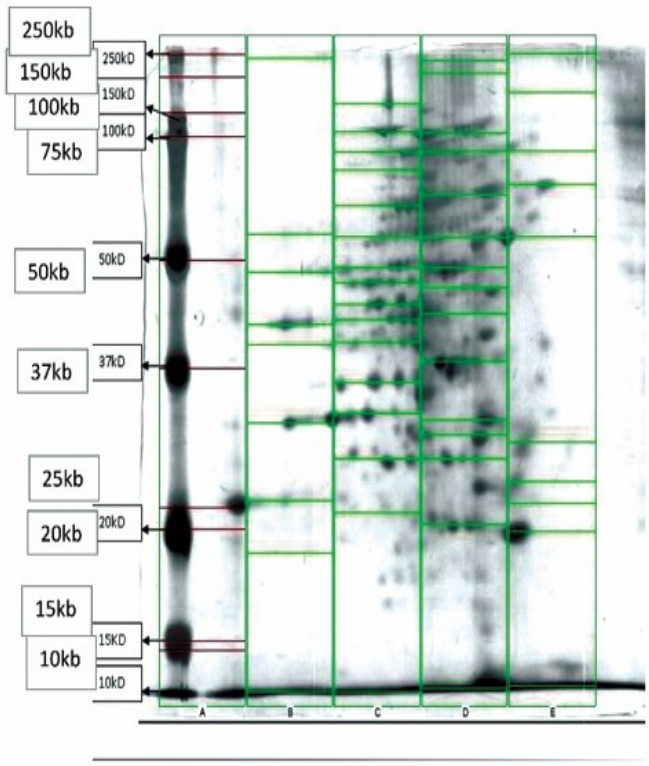
Two-dimensional electrophoretic proteomic profiling analysis of *S. auriculata* and *M. pudica* subjected to UV-B stress revealed a strong interspecific divergence in molecular responses to abiotic stress (Figs. 3–6). Spot detection and quantification were carried out using gel analysis software and the relative spot volume was normalised to the total gel spot intensity. All experiments were performed in triplicate. Only protein spots showing a change of ≥ 1.5-fold and $p \leq 0.05$ were considered significantly differentially expressed.

It was observed that the protein spot distributions of both species under the control (non-stress) treatment were mainly concentrated within the 15–75 kDa molecular mass range. However, *S. auriculata* exhibited significantly more protein spots and a higher total normalised spot volume than *M. pudica* ($p \leq 0.05$), particularly in the 48–63 and 25–37 kDa regions. This suggests a relatively more intricate and basally active metabolome in *S. auriculata*. Conversely, only a limited number of protein spots were detected in *M. pudica* and substantially lower overall spot intensities were observed under well-watered



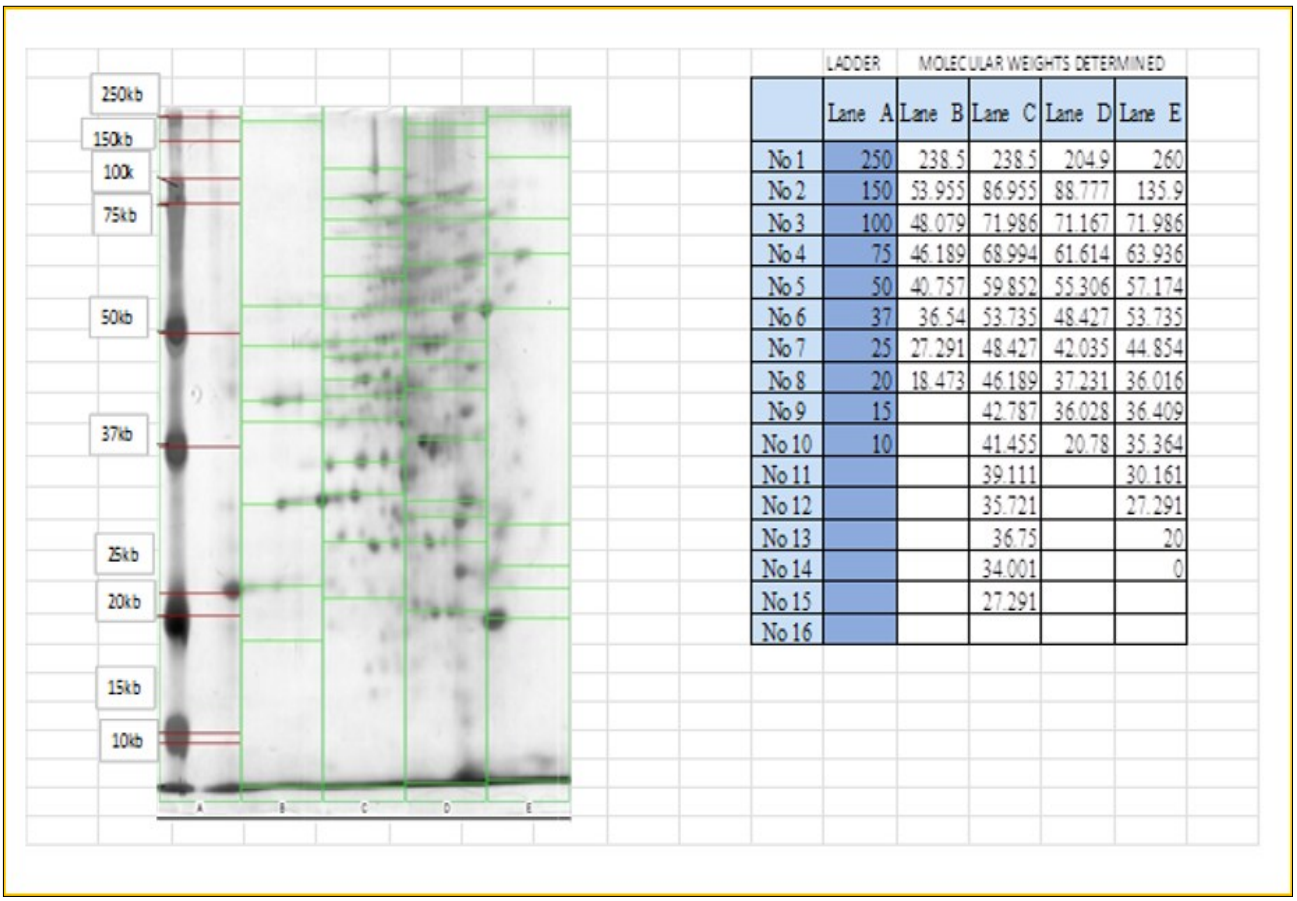
	LADDER	MOLECULAR WEIGHTS DETERMINED			
	Lane A	Lane B	Lane C	Lane D	Lane E
No 1	250	230.838	230.838	230.838	230.838
No 2	150	198.12	63.438	75	74.192
No 3	100	53.028	52.843	68.32	67.534
No 4	75	49.925	50.303	63.438	62.693
No 5	50	48.288	48.035	58.419	58.875
No 6	37	39.274	42.618	54.571	54.372
No 7	25	24.862	39.691	51.602	48.855
No 8	20	19.37	29.5	49.244	45.412
No 9	15	16.366	24.312	47.861	43.093
No 10	10	14.703	15.603	45.045	24.45
No 11			13.997	42.618	20.221
No 12			11.469	35.27	17.207
No 13				16.845	16.041
No 14				16.169	14.231
No 15				14.94	
No 16				13.126	

Fig. 3. Analysis of *Mimosa pudica* proteins by two-dimensional gel electrophoresis. A 30 µL aliquot of protein extracted from leaf tissues of *M. pudica* sample was diluted to 300 µL with rehydration buffer. The separated proteins can then be visualised by staining with a protein dye, silver stain. Molecular weights of the observed bands were determined by quantification using gel documentation.



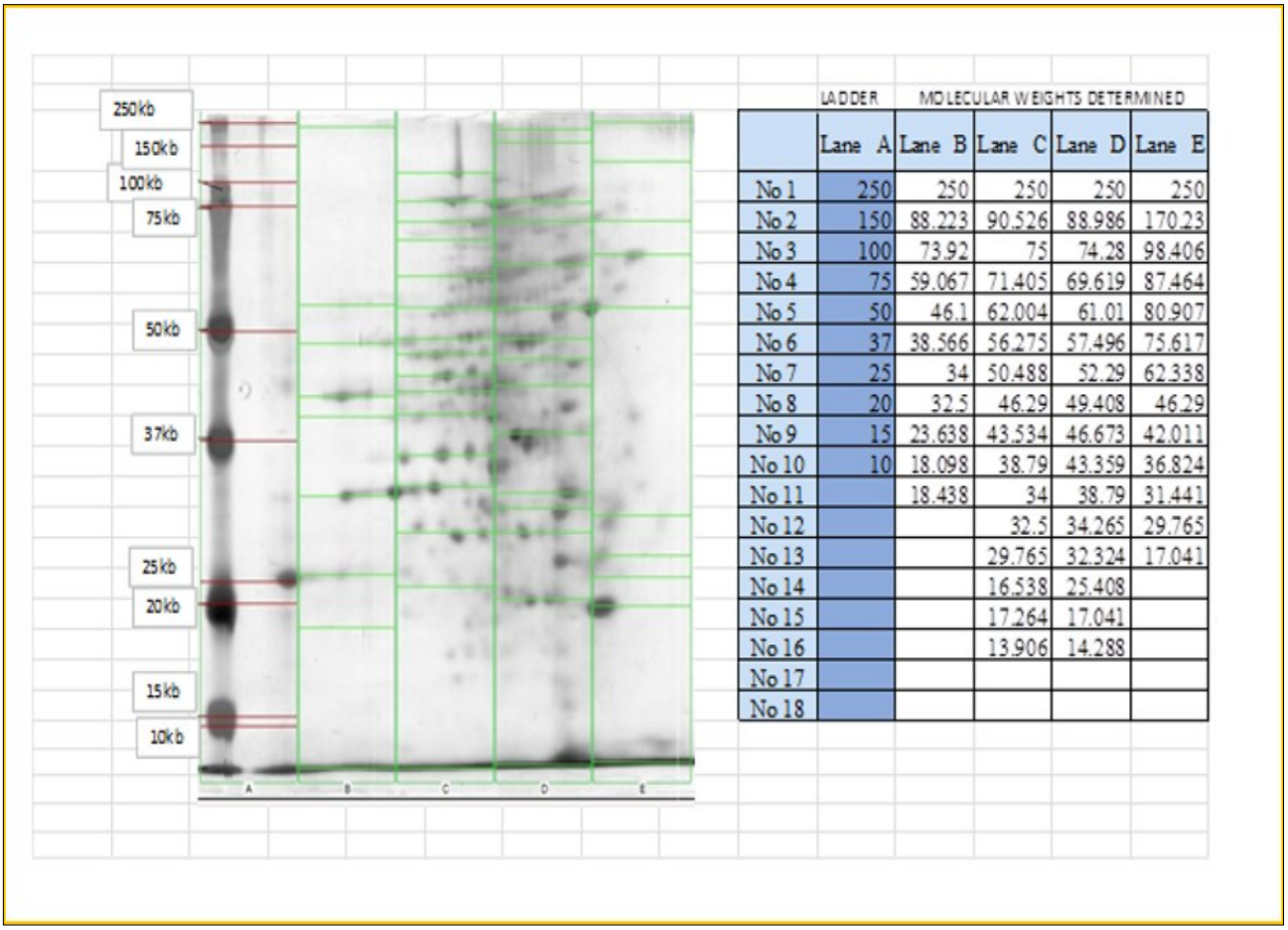
	LADDER	MOLECULAR WEIGHTS DETERMINED			
	Lane A	Lane B	Lane C	Lane D	Lane E
No 1	250	120.833	150	107.98	100
No 2	150	70.884	72.595	72.938	71.91
No 3	100	46.028	59.138	60.989	56.764
No 4	75	39.209	48.996	49.498	46.842
No 5	50	36.814	46.678	45.706	45.386
No 6	37	36.252	44.13	45.546	40.426
No 7	25	28.429	39.442	40.047	37.155
No 8	20	24.072	37.155	37.85	36.883
No 9	15		36.779	36.905	35.915
No 10	10		36.333	36.408	26.811
No 11			27.985	27.985	22.863
No 12			24.69	17.735	17.804
No 13			17.363	17.462	
No 14			17.481	16.092	
No 15					

Fig. 4. Analysis of *Mimosa pudica* proteins by two-dimensional gel electrophoresis. A 30 µL aliquot of protein extracted leaf tissues of *M. pudica* ultraviolet-B treated samples were diluted to 300 µL with rehydration buffer. The separated proteins were then visualised by staining with a protein dye, silver stain. Molecular weights of the observed bands were determined by quantification using gel documentation.



	LADDER	MOLECULAR WEIGHTS DETERMINED			
	Lane A	Lane B	Lane C	Lane D	Lane E
No 1	250	238.5	238.5	204.9	260
No 2	150	53.955	86.955	88.777	135.9
No 3	100	48.079	71.986	71.167	71.986
No 4	75	46.189	68.994	61.614	63.936
No 5	50	40.757	59.852	55.306	57.174
No 6	37	36.54	53.735	48.427	53.735
No 7	25	27.291	48.427	42.035	44.854
No 8	20	18.473	46.189	37.231	36.016
No 9	15		42.787	36.028	36.409
No 10	10		41.455	20.78	35.364
No 11			39.111		30.161
No 12			35.721		27.291
No 13			36.75		20
No 14			34.001		0
No 15			27.291		
No 16					

Fig. 5. Analysis of *Senna auriculata* proteins by two-dimensional gel electrophoresis. A 30 µL aliquot of protein extracted leaf tissues of *S. auriculata* control samples were diluted to 300 µL with rehydration buffer. The separated proteins can then be visualised by staining with a protein dye, silver stain. Molecular weights of the observed bands were determined by quantification using gel documentation.



	LADDER	MOLECULAR WEIGHTS DETERMINED			
	Lane A	Lane B	Lane C	Lane D	Lane E
No 1	250	250	250	250	250
No 2	150	88.223	90.526	88.986	170.23
No 3	100	73.92	75	74.28	98.406
No 4	75	59.067	71.405	69.619	87.464
No 5	50	46.1	62.004	61.01	80.907
No 6	37	38.566	56.275	57.496	75.617
No 7	25	34	50.488	52.29	62.338
No 8	20	32.5	46.29	49.408	46.29
No 9	15	23.638	43.534	46.673	42.011
No 10	10	18.098	38.79	43.359	36.824
No 11		18.438	34	38.79	31.441
No 12			32.5	34.265	29.765
No 13			29.765	32.324	17.041
No 14			16.538	25.408	
No 15			17.264	17.041	
No 16			13.906	14.288	
No 17					
No 18					

Fig. 6. Analysis of *Senna auriculata* proteins by two-dimensional gel electrophoresis. A 30 µL aliquot of protein extracted from leaf tissues of *S. auriculata* ultraviolet-B treated samples were diluted to 300 µL with rehydration buffer. The separated proteins were then visualised by staining with a protein dye, silver stain. Molecular weights of the observed bands were determined by quantification using gel documentation.

conditions, indicating lower baseline proteomic diversity.

After UV-B treatment, proteomic analysis revealed a comprehensive and statistically significant reorganisation of the proteome in *S. auriculata.* Out of 16 differentially expressed protein spots, 12 showed significant upregulation (1.5–2.8-fold; $p \leq 0.05$) and four were downregulated (≥1.5-fold decrease; $p \leq 0.05$). Major upregulated spots were observed at 230.83, 74.19, 63.43 and 58.87 kDa. These high molecular weight proteins may represent structural proteins, large enzymatic subunits or stress-related chaperones such as members of the HSP family; however, such assumptions require verification through mass spectrometric identification.

A noticeable induction of LMW proteins (ranging from 16.84 to 20.22 kDa) was also detected (up to 2.3-fold; $p \leq 0.01$). Some of these proteins could be related to antioxidant and redox regulation, implying that protective mechanisms were turned on to abate the UV-B-mediated oxidative stress. In contrast, the proteins with reduced expression were mainly found in the 10–15 kDa and 30–45 kDa regions ($p \leq 0.05$), signifying a targeted diminution of proteins perhaps playing a part in growth, primary metabolism, or photosynthesis that were susceptible to the environmental stress.

On the other hand, *M. pudica* showed a relatively mild proteomic response. A total of nine protein spots were significantly changed in response to UV-B, six of them were upregulated (1.4–2.0-fold; $p \leq 0.05$) and three were downregulated (≥1.5-fold decrease; $p \geq 0.05$). The upregulated proteins were mainly confined to the 49–72 kDa range, such as spots around 72.59, 59.14 and 49.47 kDa. Meanwhile, the spot intensities ($p \leq 0.05$) were much weaker than those in *S. auriculata*, suggesting lower proteomic plasticity.

Drastic downregulation was detected at 40.42, 26.81 and <20 kDa ($p \leq 0.05$), implying the depression of some housekeeping or metabolic proteins in response to long-term UV-B stress. In general, the level of fold changes and the number of DAPs were both dramatically higher in *S. auriculata* than in *M. pudica* (two-way ANOVA, $p \leq 0.05$).

Gel documentation and densitometric analyses also corroborated that protein alteration in response to UV-B was more extensive and dynamic in *S. auriculata*, whilst fewer and milder changes were observed in *M. pudica.*

The comparative features of proteomic changes between the two species are summarised in Table 1. *Senna auriculata* exhibits a wide spectrum and highly dynamic proteomic response to UV-B irradiation, comprising upregulation of high- and low-molecular weight proteins associated with structural integrity, protection of proteins, avoidance of oxidative stress and reorientation of metabolism. Such a process points to an effective cellular plan of survival and adjustment to oxidative and photodamage caused by UV-B. In contrast, *M. pudica* evinces relatively minor proteomic reorganisation, wherein fewer adapting proteins are synthesised and to an overall lesser induction. Such may be an indication of a smaller metabolism or a more cautious stress response process.

These findings demonstrate that *S. auriculata* possesses superior UV-B stress tolerance, attributed to its rapid activation of diverse stress-responsive proteins, effective redox homeostasis and strategic reallocation of energy toward survival. The contrasting proteomic responses of the two species underscore an evolutionary divergence in stress adaptation and offer valuable insights for identifying biomarkers and targets to improve stress tolerance in other plants.

Discussion

This study examines the proteomic responses of *M. pudica* and *S. auriculata* to UV-B stress using SDS-PAGE and two-dimensional gel electrophoresis (2-DE). The findings demonstrate distinct species-specific strategies for managing UV-B-mediated oxidative stress, with divergence evident in the timing and intensity of changes in protein expression. These patterns are consistent with previous studies and emphasise the critical importance of the rapid activation of protective mechanisms to counteract oxidative damage (17–19).

In *S. auriculata*, the SDS-PAGE profiles assessed early proteomic response to UV-B exhibited strong proteomic response, with significant protein upregulation in the 25–50 kDa molecular weight range as early as Day 20. These proteins are likely to comprise ATP synthase subunits, components of the oxygen-evolving complex (e.g. OEC33), Cu/Zn-SODs and PSII associated proteins, which are essential for energy production, redox system and photosynthetic stability (20). In addition, the continuous upregulation of proteins in the 15-20 kDa range, glutathione S-transferases (GSTs) and small heat shock proteins (sHSPs), suggested the activation of detoxification and chaperone systems necessary for maintaining redox homeostasis and proper protein

Table 1. Comparative proteomic responses to ultraviolet-B radiation in *Senna auriculata* and *Mimosa pudica*

Parameters	*Senna auriculata* (control)	*Senna auriculata* (UV-B)	Fold charge	*Mimosa pudica* (control)	*Mimosa pudica* (UV-B)	Fold charge	Significance
Total detected protein spots	82 ± 3	98 ± 4	1.20↑	64 ± 22	70 ± 3	1.09↑	–
No. of upregulated spots	–	12 ± 1	1.5–2.8↑	–	6 ± 1	1.4–2.0↑	–
No. of downregulated spots	–	4 ± 1	≥1.5↓	–	3 ± 1	≥1.5↓	–
Mean spot intensity (relative units)	0.86 ± 0.05	1.42 ± 0.08	1.65↑	0.74 ± 0.04	1.02 ± 0.06	1.38↑	–
Molecular weight distribution (kDa)	15–75	13–230	Broad expansion	15–75	150–15	Moderate expansion	–
Major responsive zones (kDa)	48–63, 25–37	63–75, 25–40. <20	Strong induction	40–60	40–70, <40	Moderate expansion	–

Values are expressed as mean ± SD (n = 3 biological replicates). Fold change calculated from normalised spot intensities indicates statistically significant difference at $p \leq 0.05$. UV-B: ultraviolet-B.

folding during stress (21). The early physiological and coordinated proteomic changes observed in *S. auriculata* corresponded with the stress-tolerance traits reported previously. This finding supports the presence of a preconditioned and relatively efficient defence mechanism against UV-B damage prior to stress exposure and is consistent with the rapid proteomic changes reported in other UV-B-tolerant organisms (22–24).

Two-dimensional electrophoresis (2-DE) also illustrated and further highlighted, the complexity of proteomic changes associated with UV-B stress. *S. auriculata* showed a pronounced increase in protein spots within the 25–75 kDa range, with isoelectric points (pI) between 4.5 and 7, suggesting that UV-B exposure enhanced both the number and intensity of expressed proteins (20). This pattern indicates the possible occurrence of post-translational modifications or the induction of protein isoforms involved in carbon metabolism, stress signalling and photosynthetic regulation. Additionally, the presence of protein spots exclusive to UV-B treatment suggests de novo protein synthesis in response to stress. The observed upregulation of proteins linked to reactive oxygen species (ROS) detoxification and energy metabolism pathways reflects a coordinated defence mechanism that supports survival under UV-B stress (25). These findings are consistent with reports in other plant species, where UV-B exposure induces diversification of protein isoforms associated with oxidative stress responses and energy regulation (21). However, the absence of MALDI-TOF or LC-MS/MS validation limits definitive protein identification and this should be taken into account when interpreting the proposed functional roles (17).

That noted, in *M. pudica*, 2-DE analysis undertaken at the time of UV-B stress indicated two distinct spots at the earlier time points. However, by the Days 30–40, there appeared to be more visible protein spots and a higher number of new spots appearing in the high-molecular weight (60–100 kDa) region that could have included chaperons, metabolic enzymes and structural proteins. Although the indicated overall protein diversity and intensity of the analysed spots were relatively lower than those of *S. auriculata*, it suggests that the capacity for proteomic remodelling in *M. pudica* may be less efficacious or occur at a slower rate (26). The downregulation of proteins in the size range of 10–15 kDa in both species further confirms the notion that UV-B stress generally downregulates growth-related or non-essential processes and diverts cells to protective and reparative processes. This finding is consistent with studies showing that UV-B stress typically downregulates growth-related proteins while enhancing the expression of stress-responsive proteins (17, 19). *S. auriculata* demonstrated a rapid and multifaceted proteomic response to UV-B stress, contributing to enhanced stress resistance, while *M. pudica* displayed a more restrained response, likely associated with long-term acclimatory adaptation. Furthermore, with distinct regulation of specific protein groups it is clear that early defence activation is important for enhanced UV tolerance and since this research identified potential biomarkers and stress-responsive proteins for future biotechnology approaches for crop improvement, it coincides with previous studies on the salient effects of timely UV-B stress responses on tolerance mechanisms in plants (19, 20).

Conclusion

This study provides compelling proteomic evidence of distinct ultraviolet-B (UV-B) stress adaptation strategies in *Senna auriculata* and *Mimosa pudica*, revealing a novel, timing-dependent divergence in stress-responsive protein regulation. Sodium dodecyl sulfate-polyacrylamide gel electrophoresis (SDS-PAGE) and two-dimensional gel electrophoresis (2-DE) demonstrated that *S. auriculata* quickly and co-ordinately induces proteins involved in antioxidant defence, photosynthetic stabilisation, energy metabolism and protein folding, whereas *M. pudica* exhibits a delayed and cumulatively adaptive proteomic response. A key novel finding is the early activation of low-molecular weight antioxidants and chaperones in *S. auriculata*, which strongly correlates with enhanced UV-B tolerance, while both species repress growth-associated low-molecular weight proteins, providing clear evidence for stress-induced metabolic reallocation from growth to defence. Although protein identities were inferred primarily from molecular weight and known functional associations and the analysis was limited to leaf tissues under controlled conditions without mass spectrometry validation, the strong concordance between SDS-PAGE and 2-DE datasets robustly supports the conclusion that the timing and breadth of proteomic responses are critical determinants of UV-B resilience. These findings identify *S. auriculata* as a valuable proteomic model and highlight candidate stress-responsive proteins as potential biomarkers and targets for the development of UV-B-tolerant crops.

Acknowledgements

The authors would like to thank the Principal of Pachaiyappa's College, Chennai, for providing the necessary facilities to conduct this work.

Authors' contributions

NS designed the study framework, provided guidance and validation and reviewed and edited the manuscript. PJPSM assisted in designing the experiments, developing protocols, conducting fieldwork and collecting data. SM designed experiments and protocols, conducted fieldwork, collected data and performed validation. IRS and RVK critically reviewed and revised the manuscript for important intellectual content. MS critically reviewed and revised the manuscript for important intellectual content. All authors have read and approved the final manuscript.

Compliance with ethical standards

Conflict of interest: Authors do not have any conflict of interest to declare.

Ethical issues: None

References

1. Jansen MAK, Gaba V, Greenberg BM. Plant responses to UV-B radiation: from molecular mechanisms to stress tolerance. Physiologia Plantarum. 2019:1–11.
2. Bandurska H, Niedziela J, Chadzinikolau T. The role of UV-B in plant responses to abiotic stress. Plant Physiology Reports. 2020;25:131–46.
3. Hideg É, Jansen MAK, Strid Å. UV-B exposure, ROS and stress: inseparable companions or loosely linked associates? Trends in

Plant Science. 2013;18(2):107–15. https://doi.org/10.1016/j.tplants.2012.09.003

4. Zhang Y, Zhang Y, Duan J, Liu C, Wang J, Zhai H, et al. Multi-omics analysis reveals UV-B stress tolerance mechanisms in plants. Frontiers in Plant Science. 2021;12:673381.
5. Kosová K, Vítámvás P, Prášil IT. Proteomics of stress responses in wheat and barley—search for potential protein markers of stress tolerance. Frontiers in Plant Science. 2011;2:114.
6. Righetti PG, Boschetti E. The art of observing proteome changes by electrophoretic means. Journal of Proteomics. 2020;225:103845.
7. Braam J. In touch: plant responses to mechanical stimuli. New Phytologist. 2005;165:373–89. https://doi.org/10.1111/j.1469-8137.2004.01263.x
8. Fromm J, Lautner S. Electrical signals and their physiological significance in plants. Plant Cell and Environment. 2007;30:249–57. https://doi.org/10.1111/j.1365-3040.2006.01614.x
9. Holm LG, Plucknett DL, Pancho JV, Herberger JP. The World's worst weeds. Honolulu: University Press of Hawaii; 1977.
10. Sharma P, Dubey RS. Oxidative stress and antioxidative defense system in plants. Journal of Agronomy and Crop Science. 2005;191:225–39.
11. Gamble JS. Flora of the presidency of Madras. London: Adlard & Son Ltd.; 1935.
12. Kumar S, Pandey AK. Chemistry and biological activities of flavonoids. Scientific World Journal. 2013;2013:162750. https://doi.org/10.1155/2013/162750
13. Subramanian SS, Nagarajan S. Flavonoids of the leaves of *Cassia auriculata*. Phytochemistry. 1969;8:529–31.
14. Lowry OH, Rosebrough NJ, Farr AL, Randall RJ. Protein measurement with the Folin phenol reagent. Journal of Biological Chemistry. 1951;193(1):265–75. https://doi.org/10.1016/S0021-9258(19)52451-6
15. Laemmli UK. Cleavage of structural proteins during the assembly of the head of bacteriophage T4. Nature. 1970;227(5259):680–5. https://doi.org/10.1038/227680a0
16. Blum H, Beier H, Gross HJ. Improved silver staining of plant proteins, RNA and DNA in polyacrylamide gels. Electrophoresis. 1987;8(2):93–9. https://doi.org/10.1002/elps.1150080203
17. Chaves AL, Ferreira RS, Almeida JA. Proteomic responses of *Vigna unguiculata* to UV-B stress reveal alterations in cellular redox homeostasis. Plant Physiology and Biochemistry. 2019;141:44–52.
18. Yu Z, Zheng C, Chen M. Mechanisms of UV-B radiation-induced oxidative stress in plants: insights into redox signaling and defense strategies. Journal of Experimental Botany. 2020;71(14):4137–50.
19. Singh RP, Tripathi D, Pandey SP. Proteomic insights into the stress adaptation of *Trigonella foenum-graecum* under UV-B radiation. Environmental and Experimental Botany. 2022;189:104598.
20. Hideg É, Strid Å. The effects of UV-B on photosynthesis and antioxidant defense in plants. Journal of Experimental Botany. 2023;74:3629–42.
21. Li X, Zhang H, Liu Q, Chen F. Small heat shock proteins and glutathione S-transferases coordinate redox homeostasis under UV-B stress in plants. Plant Cell Reports. 2024;43:215–29.
22. Wu D, Zhang Y, Sun Y. Comparative proteomics analysis of *Cucumis sativus* under UV-B stress and the associated mechanisms. Scientific Reports. 2021;11(1):4508. https://doi.org/10.1038/s41598-021-90633-5
23. Zhou Z, Xu Q, Liu J. Proteomic and physiological responses of *Salvia miltiorrhiza* to UV-B radiation: a focus on the regulation of antioxidant enzymes. BMC Plant Biology. 2023;23(1):15.
24. Wang R, Chen S, Zhou Y, Xu J. Rapid proteomic reprogramming confers UV-B tolerance in higher plants. Frontiers in Plant Science. 2024;15:1298743.
25. Gill SS, Tuteja N. Reactive oxygen species and antioxidant machinery in abiotic stress tolerance in crop plants. Plant Physiology and Biochemistry. 2023;196:107643.
26. Kosová K, Vítámvás P, Prášil IT, Renaut J. Proteomic responses to abiotic stress: timing, efficiency and adaptive significance. Journal of Proteomics. 2023;274:104789.

Additional information

Peer review: Publisher thanks Sectional Editor and the other anonymous reviewers for their contribution to the peer review of this work.

Reprints & permissions information is available at https://horizonepublishing.com/journals/index.php/PST/open_access_policy

Publisher's Note: Horizon e-Publishing Group remains neutral with regard to jurisdictional claims in published maps and institutional affiliations.

Indexing: Plant Science Today, published by Horizon e-Publishing Group, is covered by Scopus, Web of Science, BIOSIS Previews, Clarivate Analytics, NAAS, UGC Care, etc
See https://horizonepublishing.com/journals/index.php/PST/indexing_abstracting

Copyright: © The Author(s). This is an open-access article distributed under the terms of the Creative Commons Attribution License, which permits unrestricted use, distribution and reproduction in any medium, provided the original author and source are credited (https://creativecommons.org/licenses/by/4.0/)

Publisher information: Plant Science Today is published by HORIZON e-Publishing Group with support from Empirion Publishers Private Limited, Thiruvananthapuram, India.